RSC Advances

ROYAL SOCIETY OF CHEMISTRY

www.rsc.org/advances

Journal Name

RSCPublishing

ARTICLE

TiO_2 modified abiotic-biotic process for the degradation of azo dye methyl orange

Cite this: DOI: 10.1039/xoxxoooooox

Tingting Shen[a,b*], Chen Wang [a], Jing Sun [a], Chengcheng Jiang [C], Xikui Wang [a] and Xiaoming Li[b*]

Received ooth 2015,
Accepted ooth 2015

DOI: 10.1039/xoxxoooooox

www.rsc.org/

To investigate the feasibility of titanium dioxide (TiO_2) employed as a modifier in the sodium alginate immobilization system, the degradation of methyl orange with strain *Delftia sp. A2(2011)* were carried out in the TiO_2 modified sodium alginate system (TiO_2/SA) and non-TiO_2 modified sodium alginate system (SA), respectively. It was found that the decolorization of methyl orange was enhanced from 76.5% to 100%, and chemical oxygen demand (COD) removal was increased from 35.6 % to 52.7%. The results further revealed that TiO_2 played a crucial role in the cells immobilization system, and the potential modification mechanisms of dye sensitization and TiO_2-SA complex-mediated photocatalysis were investigated. Additionally, the intrinsic bright color of bacterial strain *Delftia sp. A2(2011)* could be ingeniously employed as an indicator for the degradation efficiency. This work not only opens a promising entry for developing novel cells immobilization techniques but also affords a direct and visualization treatment effect for azo dyes wastewater.

1. Introduction

It is reported that approximately 10,000 different dyes and pigments are industrially used and over 0.7 million tones of syntheticdyes are annually produced in the earth.[1,2] Among them, azo dyes are *ca*. one half of these dyes practically employed in the textile industry.[3,4,5] Therefore, decolorization of azo dye effluents has been received considerable attention in past decades due to the stability, toxicity and resistance to the aquatic and terrestrial organisms.[6,7,8]

Traditional physical or chemical techniques such as adsorption and chemical precipitation are unfavorable for the dyes treatment because these methods can generate a secondary pollution originated from organic compounds transfer [9-11]. Although advanced oxidation processes (AOPs) can oxidize a broad range of pollutants, they cannot be employed to effectively degrade azo dyes due to their relatively high cost. [12-15]

Microbial or enzymatic decolorization is known to be an eco-friendly and cost-competitive alternative to the chemical decomposition processes, but the toxic and genotoxic effects of azo dyes to microorganism restrict common biological treatments. [2,16,17] Therefore, developing novel strategies for the degradation of azo dyes are believed to be essential.

As well known, cells immobilization is a feasible technique for continuous degradation due to the high treatment efficiency, preferential retention of biomass, convenience of bacteria-substrate separation and avoidance of product inhibition, compared with those of the free cells.[18-20] In general, immobilization supports are consisted of inorganic materials and/or organic materials, such as ceramics,[21,22] agar, agarose, k-carrageenan or sodium alginate gel, [23,24] and fibers.[25]Among all the matrices, alginate extracted from macro-algae, a natural polymer, is widely used for the preparation of gel beads with low cost, higher bioactivity and mild conditions of immobilization.

The microorganisms immobilized in alginate beads have been used in hostile environments and the beads provide nutrients and appropriate conditions, such as facilitating the transfer of oxygen which is crucial for rapid hydrocarbon mineralization, to allow for rapid bioremediation in contaminated systems.[26-30] However, the dense gel layers of the sodium alginate beads can hinder mass transfer of substrates, pollutants, and degraded products. Furthermore, the resulting beads in the sodium alginate-immobilized system were relatively weak in the mechanical strength and stability, [24,31] limiting its practical application. So, the incorporation of some modifiers into alginate beads could facilitate the transport of pollutants towards both the surface and interior regions. [32]

TiO_2, as an effective photo sensitizer, has been traditionally performed as a catalyst under irradiation in abiotic process for pollutants degradation, generating strong oxidants such as HO• radicals that can quickly and non-selectively degrade organic compounds.[33-36] The promising applications of TiO_2 has been investigated in numerous fields ranging from photovoltaics and photocatalysis to photo-/electrochromics and sensors. Most of the reported cases depended not only on the properties of the TiO_2 material itself but also on the modifications of the TiO_2 material host, and on the interactions between TiO_2 and the environment.[37-41] Whereas, the application of TiO_2 as the microorganism immobilized support has been little documented and its application for biotic/abiotic degradation has not been yet described.

Therefore, the aim of the work is to explore a novel biotic/abiotic process initiated by TiO_2/SA, in which TiO_2 plays a great role in modifying the performances of the SA immobilized system. It was focused on the evaluation its feasibility for the decolorization and degradation of azo dye methyl orange. The degradation mechanisms of methyl orange were probed via scanning electron microscopy (SEM), optical images, UV-vis, IR and LC-MS analyses, and the promotion mechanisms involved in TiO_2/SA process were further elucidated.

2. Materials and methods

2.1 Materials

Methyl orange ($C_{14}H_{14}N_3NaO_3S$), H_2SO_4, NaOH, 2-propanol, anatase titanium dioxide (TiO_2, a surface area of *ca.* 6.6 m^2/g), SA($(C_6H_7NaO_6)n$ with mean molecular weight of 500 kDa, the particle size less than 200-mesh, and the ratio of mannuronate residues to guluronate residues (M/G) is 0.50), ammonium acetate, and the reagents used for bacterial medium, all purchased from Sinopharm Chemical Reagent Co., Ltd., China, were of analytical grade; methanol and acetonitrile were of chromatographic purity grade. All the reagents were used as received.

The applied basal medium contained the following composition: per liter of ultra-pure water, 2.5 g CH_3COONa, 0.6 g KH_2PO_4, 0.9 g K_2HPO_4, 0.075 g $CaCl_2{\cdot}2H_2O$, 0.20 g yeast extract, 0.40 g $MgCl_2$, 0.36 g NH_4Cl, 0.24 mg $ZnSO_4{\cdot}7H_2O$, 2.8 mg H_3BO_3, 0.75 mg $Na_2Mo_4{\cdot}2H_2O$, 11.8 mg $FeSO_4{\cdot}7H_2O$, and 0.04 mg $Cu(NO_3)_2{\cdot}3H_2O$. After adjusting the pH to 7.0 with 1.0 mol/L NaOH, the medium and the vessel were sterilized at 121°C for 30 min. Ultra-pure water was provided by a Milli-Q system (Millipore).

2.2 Microorganism

The strain *Delftia sp. A2(2011)* used in the work was isolated from the activated sludge of the urban sewage treatment plant in Changsha, China, according to the following method: sludge samples were agitated to obtain homogeneous suspensions in 0.9% sterile NaCl. 1 mL suspensions were pipetted into a 10 mL screw-cap tube. The tube was then completely filled with the basal medium and tightly closed in order to keep in microaerophilic condition with dissolved oxygen (DO) of 0-0.5mg/L. The incubation was performed at 30°C under illumination intensity at 3000 lux until the culture medium turned to bright red, indicated a large amount of bacteria cells produced. The bacteria cells harvested from the reactor were further cultivated in a batch culture fed with basal containing 500 mg/L methyl orange as carbon source. Strain was isolated on solid media consisting of basal medium, 1.5% agar and 500 mg/L methyl orange, which were added as a sterile solution to the autoclaved media. Colonies exhibiting strong growth were re-streaked additional six times and then placed into basal medium containing methyl orange for storage. Transfers into fresh medium were carried out at weekly intervals. The observation under microscope indicated that strain *Delftia sp. A2(2011)* formed a red colony on facultative anaerobic medium, and the cells of the strain were Gram-negative, and short-rod with flagellum. The optimum conditions of cells growth and biodegradation were investigated as pH 7.0, illumination intensity 3000 lux (the light source used in the work was an incandescent lamp, which had mixed wavelengths at the range of 400-780 nm), temperature 30°C, and DO 0-0.5 mg/L. The complete sequence of the 1454 bp 16S rDNA fragment form of *Delftia sp. A2(2011)* had been deposited in the Gene Bank database under accession number HQ659695.

2.3 Cells immobilization

The immobilization process was conducted according to the immobilization procedure that presented by Nagadomi et al. [21-22] with some revisions.

The wet cells for immobilization were harvested at the end of the exponential growth phase. The weight of the initial wet mass of the cells was fixed at 2.0 g, which were harvested by centrifugation of 400 mL cells suspension (OD_{590} = 1.5) for 15 min with the speed of 5000 rpm. The procedure of TiO_2/SA support was prepared as follows: 35.0 g/L aqueous solution of SA was first prepared by stirring 8.75 g SA in 250 mL ultra-pure water for 24 h. A required amount of TiO_2 was taken in 10 mL water separately and sonicated for 2 h, and then TiO_2 dispersion was added to the SA aqueous solution stirred overnight. The mixture was further sonicated to drive off bubbles and autoclaved for 2 min and cooled down to room temperature.

The immobilized cell beads was prepared by extrusion spheronization: the harvested cells were taken in the prepared support TiO_2/SA and stirred carefully to remain a homogenous condition, and the mixture were directly dropped into 4% (*w/v*) $CaCl_2$ with 50-mL disposable syringe at 10 cm height from the liquid level. The resulting beads with diameter of 3.0-4.0 mm were then held for 24 h at 4°C to harden the immobilization. To achieve the optimal immobilization conditions, TiO_2 quantity (1.0, 1.5, 2.0, 2.5, and 3.0 g/L), and the mass of wet cells to immobilization support (C:IS, 1:5, 1:10,1:20, 1:30, and 1:40, *w/v*) were investigated, respectively. The immobilized beads were washed with sterile water twice and divided into nine aliquots for the degradation experiments. The control experiments in SA immobilized system were conducted under the same conditions of TiO_2/SA.

2.4 Degradation experiments

Degradations of methyl orange using *Delftia sp. A2(2011)* were carried out in the following systems: TiO_2/SA, SA, free cells and free cells suspended with TiO_2. Continuous degradation experiments on methyl orange were carried out in order to investigate the continuous biodegradation of the immobilized beads. At the end of each running cycle, the degraded effluent was discharged and the immobilized beads were washed twice with sterile water, and the wet biomass was determined by weighing the immobilized cell beads after being dried by sterile filter paper in a clean bench (SWCJ1FD, Antai, Jiangsu) before and after the responding running cycle. All degradation experiments were carried out in triplicate in 250 mL tapered conical flasks that contained 10 mL culture medium. In the free cells system, the same amount of wet free cells was instead of immobilized beads for the degradation. Methyl orange (1000 mg/L) was degraded for 96 h; during the degradation process, the decolorizaton and COD_{Cr} treatment efficiency were measured by potassium dichromate ($K_2Cr_2O_7$) method [44] at the interval of 12 h.

To investigate the degradation mechanisms, control experiments in the absence of *Delftia sp. A2(2011)* of TiO_2 in dark; TiO_2 under irradiation; SA beads in dark; SA beads under irradiation; TiO_2/SA beads in dark and TiO_2/SA beads under irradiation were further investigated.

2.5 HO· scavenging and verification studies

Investigation on HO· scavenging and verification was according to literature.[42, 43]. 2-propanol was used as the scavenger. The molar ratio of scavenger to TiO_2 was 50:1. The degree of methyl orange degradation was verified by evaluating the decolorization and COD removal efficiency.

2.6 Analysis

The samples used for COD analysis were collected by centrifuging at 10,000 rpm for 20 min to remove the free cells. COD measurement was conducted according to Standard Methods. [44] pH was adjusted **to** 7.0 by 1.0 mol/L H_2SO_4 or 1.0 mol/L NaOH and measured by a pH meter (pH330i, WTW Germany). DO was controlled with N_2 flows and measured with a DO detector (Oxi300i, WTW Germany). The samples for SEM were prepared by freeze-drying the corresponding harvest cells and immobilized support (TiO_2, SA) under vacuum with -45°C. The degraded effluent for UV-vis and IR spectra should

be first dried by freeze-drying under vacuum with -45°C, and the resulting solids were then dissolved in methanol to remove inorganic matter and filtered by a Millipore filter (pore size of 0.22 μm), and dried again by freeze-drying under vacuum with -45°C. IR spectra were performed on Perkin Elmer FTIR spectrophotometer (USA) in KBr pellet. The samples for UV-vis spectra and LC-MS should be further dissolved in ultrapure water. UV-vis spectra detection was analyzed using a UV-vis spectrophotometer (UV2550, Japan) with a 1-cm quartz cell.

The samples for LC-MS detection were taken out from the fourth running cycle with the maximum degradation efficiency in the TiO_2/SA immobilized system. LC-MS were conducted on Thermo Finnigan LCQ-Advantage (USA) referring to the method presented by Baiocchi et al. [3] HPLC analyses were carried out under isocratic conditions using a RP-C18 column (Lichrospher RP-18, 250 mm × 4.6 mm; 5 mm particles, Merck, Darmstadt, Germany) and the mobile phase was composed of 10 mM acetonitrile-ammonium acetate of pH 6.8 (20/80 (*v*/*v*)), flow rate was 0.8 mL/min. The eluent from the chromatographic column could successively enter the UV-vis diode array detector, the ESI interface and the dual ion trap mass analyzer. Electrospray ionization (ESI) in negative mode with dual sprayers of ion trap MS source, detailedly operated in drying gas of 6.0 L min^{-1}, gas temperature of 300°C, nebulizer of 1 kPa, ion current control of 150,000, maximum accumulation time of 50 ms, scan of 100-325, cone gas flow of 55 L/h, desolvation temperature of 300°C, ion source temperature of 100°C, desolvation gas flow of 400 L/h, and capillary of 3800 V.

A SEM equipped with energy dispersive Spectrometer (EDS) (Quanta 200, FEI, Germany) was used to characterize the immobilized beads for their basic constituents and morphological information.

2.7 Statistical analysis

To ensure the accuracy of test data, each experiment was performed in triplicate within (±10%) data deviation to ensure reproducibility. The average values were used in the analysis.

3. Results and discussion

3.1 Optimum conditions investigations for the degradation of methyl orange

Figure 1 was the biodegradation kinetics of methyl orange by free *Delftia sp. A2(2011)* at different initial concentrations. The result showed that methyl orange could be completely decolorized with the initial concentrations of 100 mg/L and 500 mg/L, while apparently decreased when the initial concentration increased to 1000 mg/L. Therefore, in contrast to the free *Delftia sp. A2(2011)*, 1000 mg/L of methyl orange was chosen as the basal concentration in the cells immobilization system.

To achieve the optimal immobilization conditions, the quantity of TiO_2 and the mass of wet cells to immobilization support (C:IS, *w*/*v*) were investigated. In Fig. 2a, with the increasing quantity of TiO_2, the treatment efficiency gradually increased until the quantity of TiO_2 was enhanced to 2.0 g/L. But instead, the treatment efficiency decreased when loaded TiO_2 was more than 2.0 g/L. It could be ascribed that the dense gel layers of the TiO_2/SA beads could hinder microorganism accumulation and mass/energy transfer of substrates, pollutants, and degraded products, inhibiting the cells growth and bioactivity,[30-32, 45] on the other hand, the excess quantity of TiO_2 did bactericidal effects on the cells, reducing the active biomass.[39,41] So, the optimal quantity of TiO_2 was selected as 2.0 g/L.

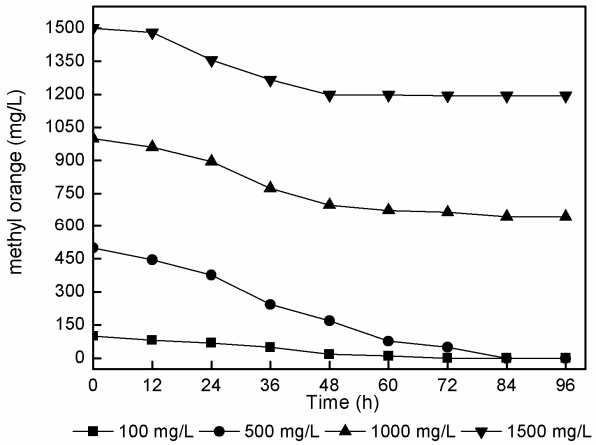

Fig. 1 Kinetics of methyl orange biodegradation by free strain *Delftia sp. A2(2011)*

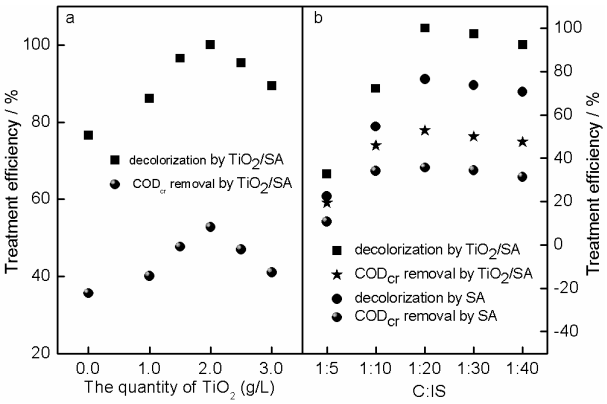

Fig. 2 The treatment efficiency with varying quantity of TiO_2 in the TiO_2/SA system (a); ratios (*w*/*v*) of C:IS in the TiO_2/SA and SA system (b), respectively. Note that C:IS is the ratio of the wet cells to immobilization support (C:IS, *w*/*v*); the quantity of TiO_2 is the mass of TiO_2 that mixed with sodium alginate (SA) as immobilization support in the TiO_2/SA system

In Fig. 2b, the optimal treatment efficiencies were obtained at the ratio of C:IS of 1:20. As immobilization support, TiO_2/SA or SA was responsible for mass and energy transfer for the immobilized cells. The inadequate loadings of C:IS (such as 1:5 or 1:10 of the ratio of C:IS) could do inhibition effect on cells growth due to the ineffective mass/energy transfer for the cells inside the beads, and thus biodegradation just carried out on the surface of the beads, decreasing bioactivity and reducing the treatment efficiency.[30-32] On the contrary, when the ratio of C:IS was changed to 1:30 or 1:40, the excess loading of TiO_2/SA or SA would cause an eutrophic environment, which also had an inhibitory effect on cells growth. Especially, the excess loading of TiO_2/SA would bring excess quantity of TiO_2, which did bactericidal effects on the cells, reducing the active biomass. [41] So the optimal ratio of C:IS was selected as 1:20.

3.2 Various processes for the degradation of methyl orange

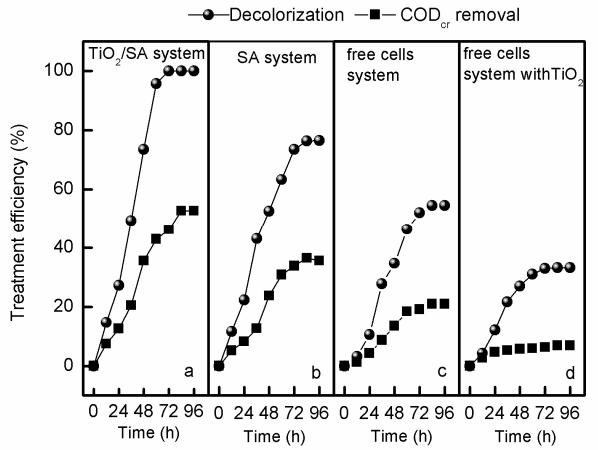

Fig. 3 Treatment efficiency of methyl orange in the TiO_2/SA system (a), SA system (b), free cells system and free cells system suspended with TiO_2 under the optimal conditions

Under the optimal conditions, the maximum decolorization and COD removal could reach 100% and 52.7% in the TiO_2/SA system, whereas to 76.5% and 35.6% in the SA system; 54.5% and 20.9% in the free cells system; 33.2% and 6.9% in the free cells system with TiO_2 (Figs. 3a-3d). As expected, TiO_2/SA system exhibited much more excellent biodegradation on methyl orange.

The control experiments in the absence of *Delftia sp. A2(2011)* were conducted simultaneously (Fig.4). The results revealed that TiO_2, irradiation and SA played a great role in degradation process. Compared with the results in Figs. 3a-3d, it was found that *Delftia sp. A2(2011)* was responsible for the large-scale treatment efficiency.

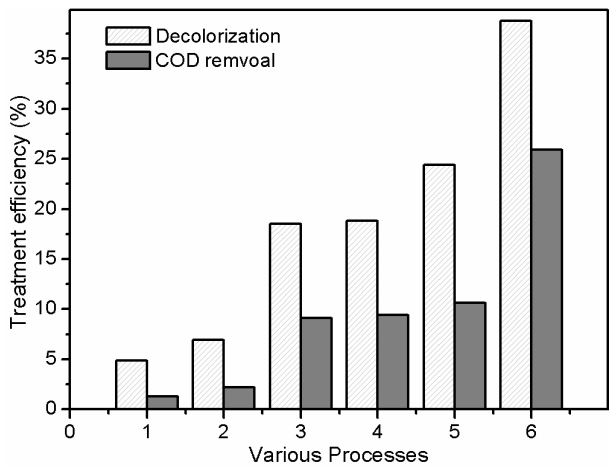

Fig. 4 Comparative treatment efficiency of methyl orange in various processes in the absence of *Delftia sp. A2(2011)* after 96 h of incubation. Noted: 1: TiO_2 in dark; 2:TiO_2 under irradiation; 3: SA beads in dark; 4: SA beads under irradiation; 5: TiO_2/SA beads in dark; 6: TiO_2/SA beads under irradiation

3.3 Degradation pathway of methyl orange in the TiO_2/SA system

Methyl orange shows two featured peaks located at 466 nm and 269 nm before treatment (Fig. 5). After 96 h of degradation, the absorption peak originated from the chromophore of N=N group (466 nm) decreased quickly, while the absorption at 269 nm originated from benzene ring simultaneously blue shifted to 245 nm, indicating that azo bond was destroyed and other degradation intermediates containing benzene ring generated. It was evident that the decolorization of methyl orange was easily achieved while the destruction of benzene ring was hardly reached.

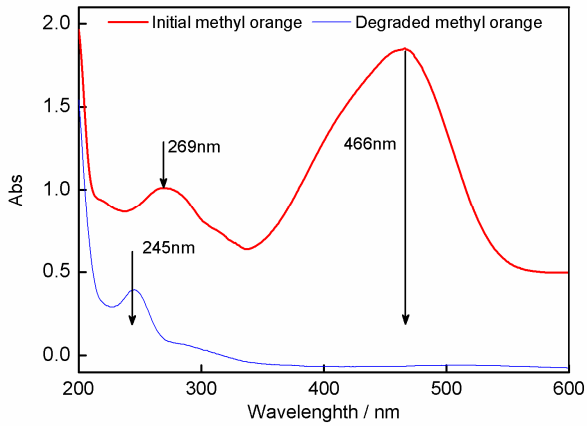

Fig. 5 UV-Vis spectra of the original and degraded methyl orange in the TiO_2/SA immobilized system

In Fig. 6, the original methyl orange exhibited peak at 3437 cm^{-1} for N–H stretching; C−H stretching vibrations of $–CH_3$ located at 2924 cm^{-1} and 2854 cm^{-1}; C−C vibration of benzene skeleton observed at 1609 cm^{-1} and 1542 cm^{-1}; N=N vibration appeared at 1421 cm^{-1}; C−N vibrations was assigned at 1369 cm^{-1} and 1194 cm^{-1}; S=O vibrations was located at 1122 cm^{-1}; C−H stretching vibrations of benzene ring were located at 1039 cm^{-1}, 847 cm^{-1}, 818 cm^{-1} and 698 cm^{-1}; C–S stretching vibrations was at 624 cm^{-1} and 575 cm^{-1}.

The degraded products of methyl orange showed the peak at 3453 cm^{-1} for N–H bend, band at 3130 cm^{-1} due to the presence of aromatic C–H bonds, which were not present in the original methyl orange but appeared in the degraded product. It could be ascribed that the conjugated double bond of N=N in the original methyl orange weakened the absorbance. This further indicated that the conjugated π-π interactions resulted from azo bond N=N was broken down.[3] Peak at 2926 cm^{-1} for asymmetric $–CH_3$ stretching vibrations; peaks at 1578 cm^{-1}, 1462 cm^{-1} for C−C vibration of benzene skeleton; 1416 cm^{-1} and 1261 cm^{-1} for C–N aromatic stretching vibrations; 1122 cm^{-1} and 1070 cm^{-1} for S=O stretching vibrations; 956 cm^{-1}, 849 cm^{-1} for aromatic C–H vibration; 575 cm^{-1} for C–S, indicated the formation of new products with sulfonated aromatic ring or benzene ring.

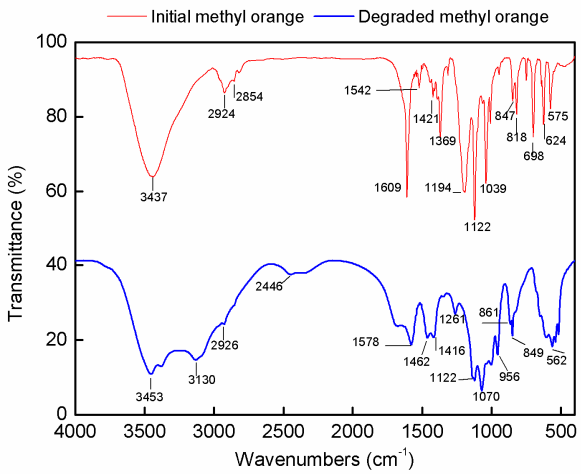

Fig. 6 IR spectra of original methyl orange and the degraded products with TiO_2/SA immobilized *Delftia sp. A2(2011)*

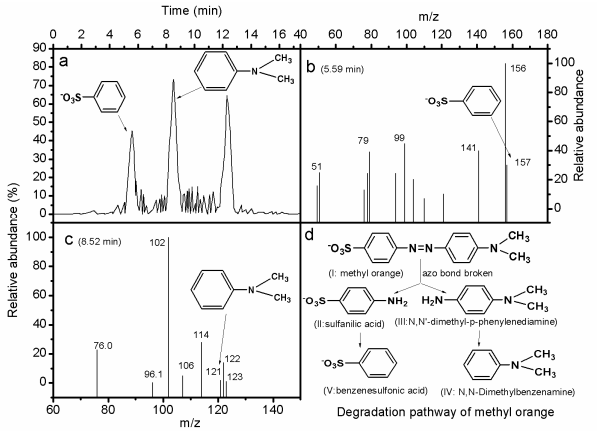

Fig. 7 LC chromatogram of the degraded methyl orange (a); the mass spectra and compound confirmation for the degradation products (b)-(c); degradation pathway of methyl orange (d)

The results were further supported by LC-MS (Fig. 7), the degraded products were separated at the retention time of 5.59 min and 8.52 min (Fig. 7a), and each peak was characterized by its mass measurements (*m/z*), respectively (Figs. 7b-c). It was concluded that the degraded pathway of methyl orange was first involved in a symmetric cleavage of azo bond yielding benzenesulfonic acid at *m/z* 157 ($C_6H_5SO_3$) (Fig. 7b). The other degradation product was N, N'-dimethyl benzenamine, which was confirmed by mass measurement at *m/z* 121 ($C_8H_{11}N$) with a characteristic fragment at *m/z* 106 (Fig. 7c). Therefore, the degradation pathway of methyl orange was potentially involved in a cleavage of azo bond, yielding benzenesulfonic acid and N, N'-dimethyl benzenamine (Fig. 7d), and then followed by further degradation or mineralization.

3.4 Characteristics in the TiO_2/SA system

Figure 8 demonstrated that the Wt% of Ti in sodium alginate was 0.46%, which increased to 16.25% in the immobilized beads after the fifth treatment. This indicated that the increasing content of Ti must come from the adding TiO_2. As shown in Figs.9a-c, the instinct cavities of TiO_2 and SA particles are full of cavities that could provide preferential pathways for microorganism accumulation and mass transfer. [26,28,31,38] Fig. 9d presented that the immobilization support was filled with zoogloea after the fifth running cycle. The results firmly demonstrated that strain *Delftia sp. A2(2011)* could not only survive in the TiO_2/SA system but also perform continuous biodegradation for methyl orange due to the appreciable removal efficiency in the five running cycles (Table 1), which could be further supported by the optical images of *Delftia sp. A2(2011)* beads immobilized by TiO_2/SA (Figs. 10a-f). It was evident that the beads immobilized by TiO_2/SA had brighter colour, performed better granular characteristics and maintained continuous biodegradation. Whereas, some of SA immobilized beads were soften and cells gradually released from the immobilized gels into the reaction liquid in the first degradation running cycle and the immobilized beads were difficult to carry out the next running cycle (Figs. 10g-h). The result indicated that beads immobilized by SA were less stable than that of TiO_2/SA. It was strongly revealed that TiO_2 could improve the mechanical strength and stability of the beads.[38,40] Fig. 10i demonstrated that the cells of *Delftia sp. A2(2011)* changed from bright red to black when TiO_2 was suspended into the free cells system, which declared that TiO_2 performed bactericidal effects on the free cells. The results were agreement with those reported in literatures. [39,41,46]

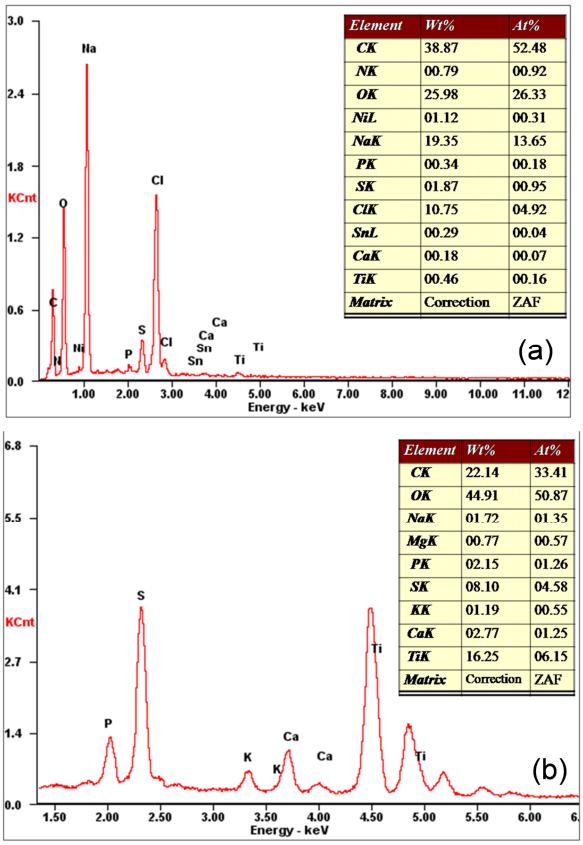

Fig. 8 Elementary analysis of the initial sodium alginate (a) and the beads in TiO_2/SA system after the fifth treatment cycle (b)

Table 1 Characteristics in the continuous running cycles

Treatment Efficiency and Biomass*	Running cycles				
	Cycle 1	Cycle 2	Cycle 3	Cycle 4	Cycle 5
COD_{cr} removal (% ±sd)	41.2±0.5	45.8±0.7	52.5±0.6	52.7±0.5	51.9±0.3
Biomass (g±sd)	30.4±0.4	32.5±0.3	35.8±0.2	37.2±0.4	37.0±0.5

* Biomass was described by the mass change of the beads after the corresponding running cycle. The initial biomass was 28.5 g; sd: standard deviation.

The biomass could be qualitatively presented by the color change of the immobilized beads (Figs. 10a-f) and quantitatively depicted by the mass change of immobilized beads before/after corresponding running cycle (Table 1), respectively. The maximum mass of immobilized beads in the TiO_2/SA system was increased from *ca.* 28.5 g to 37.2 g after five running cycles, and the biomass could be counted as *ca.* 8.7 g. So, as a modifier in the TiO_2/SA system, associated with SA, TiO_2 were responsible for mass/energy transfer, the higher mechanical strength and stability of the beads, resulting in more active biomass and higher treatment efficiency, which was in good agreement with the results reported by de-Bashan and Bashan that the increasing biomass was responsible for the increasing treatment efficiency. [45]

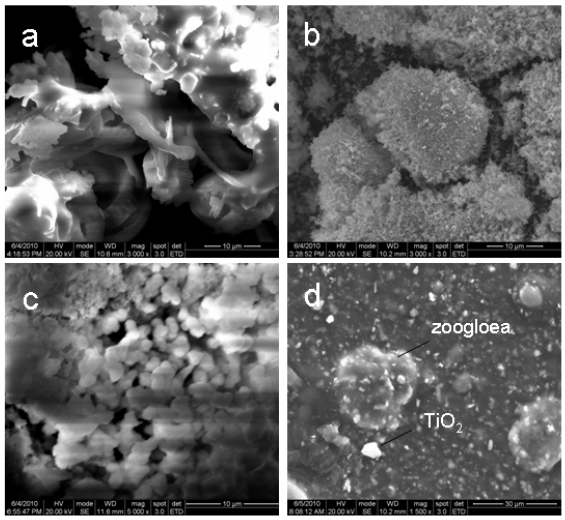

Fig. 9 SEM images of original SA (a); original TiO_2 (b); TiO_2/SA immobilized *Delftia sp. A2(2011)* before treatment (c); TiO_2/SA immobilized *Delftia sp. A2(2011)* after treated fifthly (d).

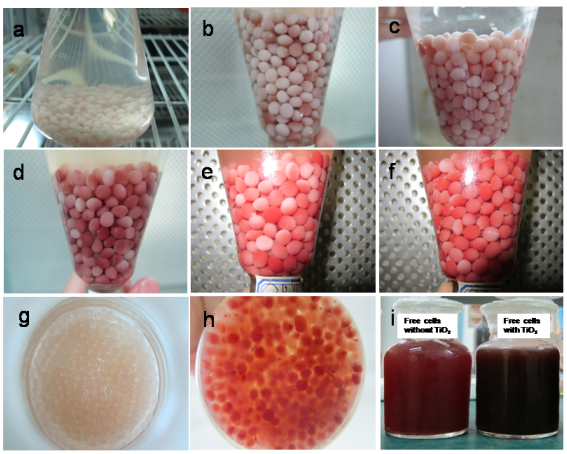

Fig.10 Optical images of strain beads immobilized by TiO_2/SA: before treatment (a); after running cycle of 1st (b); 2nd (c); 3rd (d); 4th (e); and 5th (f); Optical images of strain beads immobilized by SA: before treatment (g); after the first running cycle (h); the color of the cells in the free cells system that with/without TiO_2 (i). Note that the picture of beads (a) and (g) were taken in 4% $CaCl_2$ and the pictures of (b)-(f) were taken in the corresponding degraded effluent. The pictures of (g) and (h) were taken from the topside

3.5 Dye-sensitized promotion mechanisms in the TiO_2/SA system

As a classical semiconductor catalyst, illumination of TiO_2 with light shorter than 400 nm can generate excess electrons in the conduction band (e^-_{Cb}) and positive "holes" in the valence band (h^+_{vb}). The following photo-assisted reactions could occur: [35,36]

$$TiO_2 + h\upsilon \rightarrow e^-_{cb} + h^+_{vb} \quad (1)$$

This is followed by the formation of extremely reactive radicals (such as HO·) at the semi-conductor surface and/or direct oxidation of contaminations (R):

$$h^+_{vb} + H_2O(ads.) \rightarrow HO\cdot + H^+ \quad (2)$$

$$h^+_{vb} + OH^-(sur.) \rightarrow HO\cdot \quad (3)$$

$$h^+_{vb} + R(ads.) \rightarrow R^+ \quad (4)$$

The electros and holes may also recombine together without electron donors or acceptors:

$$e^-_{cb} + h^+_{vb} \rightarrow TiO_2 \quad (5)$$

It has been investigated in an aqueous TiO_2 dispersion under irradiation by visible light, the dyes can be easily decomposed photochemically by visible light.[49,50] Photosensitized degradation of organic dyes has been carried out on TiO_2 where the organic dye serves as both a sensitizer and a substrate to be degraded. [51-57]

And thus, in the TiO_2/SA system, the following reaction mechanisms are further proposed due to the dye sensitization effect (Eqs 6-8). That is, the electron from the excited dye molecule is injected into the conduction band of the TiO_2, and the cation radical formed at the surface quickly undergoes degradation to yield stable products: [53-55]

$$\text{Methyl orange}/TiO_2 + \text{Visible light} \rightarrow \text{Methyl orange}^*/TiO_2 \quad (6)$$

$$\text{Methyl orange}^*/TiO_2 \rightarrow \text{Methyl orange}\cdot + /TiO_2 + e^-_{cb} \quad (7)$$

$$\text{Methyl orange}\cdot + \rightarrow \text{products} \quad (8)$$

HO· scavenging studies were further conducted to determine whether the dye sensitized process was mediated by HO·. Figure 11a indicated that the decolorization and COD removal efficiency (100% and 52.7%) in the TiO_2/SA system, were decreased by 17.0% and 13.0% after addition of 2-propanol . The results indicated that HO· might be one of the active media in the TiO_2/SA system. Furthermore, Ndjou'ou et al.[43] and Howsawkeng et al.[58] had reported that it was possible for bacteria to coexist with HO· to promote simultaneous chemical and biological oxidation. Therefore, it was reasonable to deduce that TiO_2 assisted photo-catalytic process was potentially cooperated with the microbial process that contributed to the removal of methyl orange simultaneously.

Figure 11a further demonstrated that the treatment efficiency (83.0% decolorization and 39.7% COD removal efficiency) in the TiO_2/SA system with addition of 2-propanol were still 6.5% and 4.1% higher than those of the SA system (76.5% and 35.6%), and it could be deduced that other promotion mechanisms should exist.

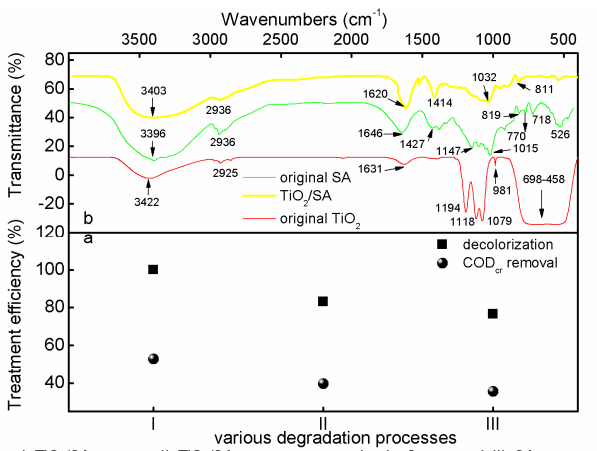

Fig.11 The comparison of treatment efficiency in TiO_2/SA system, TiO_2/SA system that scavenged by 2-propanol and SA system after 96 h degradation (a); IR spectra of original SA, TiO_2 and TiO_2/SA (b)

3.6 Complex-mediated photocatalysis mechanisms in the TiO_2/SA system

Complexation of ligand-to-metal charge transfer (LMCT), in which sensitization, electron is photo-excited directly from the highest occupied molecular orbital (HOMO) level of the adsorbate to the

TiO_2 e_{cb}, and the LMCT complexation is an easy way to extend light respond of TiO_2 to the visible region and is versatile because numerous adsorbates are potential candidates for the LMCT sensitization. A variety of organic or inorganic compounds that can form LMCT complexes on TiO_2 has been recently reviewed.[53,59]

It has been reported that the fact that TiO_2-glucose could form a LMCT complex that absorbed visible light has been recognized. [60] In the work, SA is a natural macromolecular polysaccharide $(C_6H_70_6Na)n$, which including abundant of –OH.[57,61] So it is reasonable to deduce that in the TiO_2/SA system, TiO_2 and SA could form a kind of complexation of ligand-to-metal (TiO_2-SA), and SA could serve as an electron donor for the reduction of N=N, contributing to decolorization and degradation of methyl orange.

To confirm the mechanisms LMCT occurred in our cases, the IR spectra of initial TiO_2, SA and mixture of TiO_2-SA were comparatively investigated. As shown in Figure 11b, the main bands of SA were located at 3396 cm^{-1}, 2936 cm^{-1} , 1646 cm^{-1} and 1427 cm^{-1}, 1147 cm^{-1} and 1015 cm^{-1}, which was assigned to –OH stretch vibration, C–H stretch vibration; –COO special vibration; C–O and C–H vibration of pyranoid ring; C–OH stretch vibration, respectively. The main bands of TiO_2 at 3422 cm^{-1}, 1631 cm^{-1}, 1079 cm^{-1} presented that the surface of TiO_2 was loaded with –OH. Whereas, as for the mixture of TiO_2 and SA contributed to a series of new IR peaks compared with that of alone TiO_2 or SA, and the bands at 3000 cm^{-1}–3700 cm^{-1}, 1000 cm^{-1}–1225 cm^{-1} were greatly broader than that of SA and TiO_2 alone, the result could be attributed that –OH of TiO_2 associated with the –OH, –COO and C–O of SA, which made the electron cloud density averaged, forming LMCT complex.[40,53] Moreover, it was found that the IR spectra of TiO_2/SA took red shift generally. The results further supported that LMCT complexation mechanisms was an easy way to extend light respond of TiO_2 to the visible region, [40,59,60] and thus, TiO_2/SA immobilization system was much more feasible for light harvest for cells growth than that of SA immobilized system. Therefore, in the TiO_2/SA immobilized system, TiO_2 acted as immobilization support and photo catalyst as well. Moreover, TiO_2 played a great role in enhancing the stability of sodium alginate. [31,38] The TiO_2-SA surface complex could be deduced as the following way. [53, 59, 60]

$$\text{Ti (IV)-OH} + \text{HO-C}_6\text{H}_5\text{O}_4\text{Na-OH} \rightarrow \text{Ti (IV)-O- C}_6\text{H}_5\text{O}_4\text{Na-OH} + \text{H}_2\text{O} \quad (9)$$

Besides the above mechanisms, TiO_2 and SA was potentially served as adsorbent to facilitate the transport of methyl orange and energy towards both the surface and interior regions of the immobilized beads.[31,38] And thus, it was easy to explain why TiO_2, SA and TiO_2/SA alone in dark still showed treatment efficiency for methyl orange.

4. Conclusions

In summary, TiO_2/SA process was considered to be a novel and effective strategy for methyl orange removal. Results revealed that TiO_2 played a pivot role in enhancing the characteristics of SA:

(1) Promoting the biomass production due to the formation of TiO_2-SA complex that feasible for light harvest.

(2) Enhancing the degradability and stability of the immobilized beads due to the high treatment efficiency of decolorization and COD removal in the continuous running cycles.

(3) Constructing synergetic mechanisms for the degradation of methyl orange including adsorption, biodegradation, dye sensitization and LMCT.

Additionally, the limited COD reduction could be overcome by combining TiO_2/SA and activated sludge process

Acknowledgements

This work was supported by the National Natural Science Foundation of China (Grant No. 51078128).

Notes and references

[a] *College of Environmental Science and Engineering, Qilu University of Technology, Ji'nan, 250353, P.R. China; E-mail: stthunanyt@163.com; Fax: +86-531-89631680; Tel: +86-531-89631680*

[b] *College of Environmental Science and Engineering, Hunan University, Changsha 410082, P.R. China. E-mail: xmli_2015@163.com; Tel: +86-731-8823967; Fax: +86-731-882282*

[C] *School of Chemistry and Pharmaceutical Engineering, Qilu University of Technology, Ji'nan, 250353, P.R. China.*

1 T. Robinson, G. McMullan, R. Marchant and P. Nigam, Bioresour. Technol. 2001, 77, 247-255.
2 Parshetti G. K., Telke A. A., Kalyani D. C., Govindwar S. P., J. Hazard. Mater., 2010, 176, 503-509.
3 C. Baiocchi, M. C. Brussino, E. Pramauro, A. B Prevot., L. Palmisano and G. Marci, Int. J. Mass Spectrom., 2002, 214, 247-256.
4 V. Vitor and C.R. Corso, J. Ind. Microbiol. Biotechnol. 2008, 35, 1353-1357.
5 S.Saroj, K. Kumar, N. Pareek, R. Prasad and Singh R.P., Chemosphere, 2014,107, 240-248.
6 H. Y. Zhu, R. Jiang, L. Xiao and G. M. Zeng, Bioresour. Technol., 2010, 101, 5063-5069.
7 Y. Wu, T. Li and L. Yang, Bioresour. Technol., 2012, 107, 10-18.
8 N. Boucherit, M. Abouseoud and L. Adour, J. Environ. Sci., 2013, 25, 1235-1244.
9 M. Auta and B.H. Hameed, Colloid. Surf., B: 2013,105, 199-206.
10 F. Taghizadeh, M.Ghaedi, K. Kamali, E. Sharifpour, R. Sahraie and M.K. Purkait, Powder Technol. 2013, 245, 217-226.
11 M. Ghaedi, F. Karimi, B. Barazesh, R. Sahraei, and A. Daneshfar, J. Ind. Eng. Chem., 2013**,** 19, 756-763.
12 E. Hosseini Koupaie, M.R. Alavi Moghaddam and S.H. Hashemi, Water Sci. Technol., 2013, 67, 1816-1821.
13 M. Tabatabaee, A. Ghotbifar and A.A. Mozafari, Fresenius Environ. Bull., 2012, 21, 1468-1473.
14 E. Chatzisymeon, C. Petrou and D. Mantzavinos, Global NEST J., 2013,15, 21-28.
15 Y.L. Pang and A.Z. Abdullah, Appl. Catal. B: Environ., 2013, 129, 473- 481.
16 U. Zissi and G. Lyberatos, Water Sci. Technol., 1996, 34, 495-500.
17 M. Solís, A. Solís, H.I. Peréz, N. Manjarrez and M. Flores, Process Biochem., 2012. 47, 1723-1748.
18 C. Zhang, X. Zhu, Q. Liao, Y. Wang, J. Li, Y. Ding and H. Wang, Int. J. Hydrogen Energy, 2010, 35, 5284-5292.
19 H. Ardag Akdogan and N. Kasikara Pazarlioglu, Process Biochem., 2011b, 46, 834-839.
20 H. Ardag Akdogan and N. Kasikara Pazarlioglu, Process Biochem., 2011a, 46, 840-846.
21 H. Nagadomi, T. Kitamura, M. Watanabe and K. Sasak, Biotechnol. Lett., 2000 a, 22, 1369-1374.

22 H. Nagadomi, K. Takahashi, K. Sasaki and H. C. Yang, World J. Microbiol. Biotechnol., 2000 b, 16, 57-62.
23 J. Fißler, G. W. Kohring and F. Gitthorn, Appl. Microbiol. Biotecnol., 1995, 44, 43-46.
24 K. Takeno, Y. Yamaoka and K. Sasaki, World J. Microbiol. Biotechnol. 2005, 21, 1385-1391.
25 P. Xu, X. M. Qian, Y. X. Wang and Y. B. Xu, Appl. Microbiol. Biotechnol., 1996, 44, 676-682.
26 C. J. Cunningham, I. B. Ivshina, V. I. Lozinsky, M. S. Kuyukina and J. C. Philp, Int. Biodeterior. Biodegrad., 2004, 54, 167-174.
27 C. Sathesh Prabua and A. J. Thatheyus, Int. Biodeterior. Biodegrad., 2007, 60, 69-73.
28 T. Vancov, K. Jury, N. Rice, L. Van Zwieten and S. Morris, J. Appl. Microbiol., 2007, 102, 212-220.
29 S. Bazot and T. Lebeau, Bioresour. Technol., 2009, 100, 4257-4261.
30 G. Yañez-Ocampo, E. Sanchez-Salinas, G. A. Jimenez-Tobon , M. Penninckx and M. L. Ortiz-Hernádez, J. Hazard. Mater., 2009, 168, 1554-1561.
31 Z.Y. Wang, Y. Xu, H.Y. Wang, J. Zhao, D.M. Gao, F.M. Li and B. Xing, Pedosphere, 2012, 22, 717-725.
32 K. Zhang, Y.Y. Xu, X. F. Hua, H. L. Han, J. N. Wang, J. Wang Y. M. Liu and Z. Liu, Biochem. Eng. J., 2008, 41, 251-257.
33 Y. J. Li, X. D. Li, J. W. Li and J. Yin, Water Res., 2006, 40,1119-1126.
34 K. Dai, H. Chen, T. Y. Peng, D. N. Ke and H. B. Yi, Chemosphere, 2007, 69, 1361-1367.
35 M. Huang, C. Xu, Z. Wu, Y. Huang, J. Lin and J. Wu, Dyes Pigments, 2008, 7, 327-334.
36 Y. Kim, J. Lee, H. Jeong, Y. Lee, M. H. Um, K. M. Jeong, M. K. Yeo and M. Kang, J. Ind. Eng. Chem., 2008, 14, 396-400.
37 X. Chen and S.S. Mao, Chem. Rev., 2007,107, 2891-2959.
38 J.M. Rankin, S. Baker and K.J. Klabunde, Microporous Mesoporous Mater., 2014, 190 105-108.
39 E. GilPavas, J. Acevedo, L.F. Lopez, I. Dobrosz-Gomez and M.A. Gomez-Garcia, J. Adv. Oxid. Technol.，2014, 17, 343-351.
40 K. M. Reddy, M. Sairam,; V. R. Babu, M.C.S. Subha, K. C. Rao and T.M. Aminabhavi, Des. Monomers and Polymers, 2007, 10, 297-309.
41 Q. Li, S. Mahendra, D. Y. Lyon, L. Brunet, M. V. Liga, D. Li, P. J. J. Alvarez, Water Res., 2008, 42, 4591-4602.
42 G. Buxton, C. L. Greenstoc, W. Helman, and A. B. Ross, J. Phys. Chem., 1988, 17, 513-886.
43 A. C. Ndjou'ou, B. N. Joseph and D. Cassidy, Environ. Sci. Technol., 2006, 40, 2778-2783.
44 A. D. Eaton, L. S. Clesceri and A. E. Greenberg Standard Methods for the Examination of Water and Wastewater, 19th Edition. APHA (American Public Health Association). 1995, Washington, DC, USA.
45 L. E. de-Bashanm and Y. Bashan, Bioresour. Technol., 2010,101, 1611-1627.
46 L. K. Adams, D. Y. Lyon and P. J. J. Alvarez, Water Res., 2006, 40, 3527-3532.
47 R. Didier and M. Sixto, Sci. Total Environ., 2002, 291, 85-97.
48 M. Bertelli and E. Selli, J. Hazard. Mater., 2006, 138, 46-52.
49 C. Anderson and A. J. Bard, J. Phys. Chem., 1995, 99, 9882-9885.
50 C. Nasr, K. Vinodopal, L. Fisher, S. Hotchandani, A. K. Chattopadhyay and P. V. Kamat, J. Phys. Chem., 1996, 100, 8436-8442.
51 Y. Cho, W. Choi, C. H. Lee, T. Hyeon and H. I. Lee, Environ. Sci. Technol., 2001, 35, 966-970.
52 F. Zhang, J. Zhao, L. Zang, T. Shen, H. Hidaka, E. Pelizzetti, and N. Serpone, J. Mol. Catal. A: Chem., 1997, 120, 173-178.
53 A. Hagfeldt, G. Boschloo, L.V. Sun; L. Kloo and H. Pettersson, Dye-sensitized solar cells, Chem. Rev., 2010,110, 6595-6663.
54 A.M. Al-Alwani Mahmoud, A. B. Mohamad, A. A. H. Kadhum; N. A. Ludin, Spectrochim. Acta Part A, 2015, 138, 130-137
55 S. Feng, Q.S. Li, L.N. Yang, Z.Z. Sun, T. A. Niehaus and Z.S. Li, J. Power Sources, 2015, 273, 282-289.
56 J. Wu, Z. Lan, J. Lin, M. Huang, Y. Huang, L. Fan and G. Luo, Chem. Rev., 2015, 115, 2136-2173.
57 D. R. Chejara, S. Kondaveeti and A. K. Siddhanta. Polym. Bull., 2015,72,35-48
58 J. Howsawkeng, R. J. Watts, D. L. Washington, A. L. Teel, T. F. Hess and R. L. Crawford, Environ. Sci. Technol., 2001, 35, 2961-2966.
59 G. Zhang, G. Kim and W. Choi, Energy Environ. Sci., 2014, 7, 954-966.
60 G. Kim, S. H. Lee and W. Choi, Appl. Catal., B, 2015, 162, 463-469.
61 N. Nagasawa, H. Mitomo, F. Yoshii and T. Kume, Polym. Degrad. Stab., 2000, 69, 279-285.

